ce/papers
The online collection for conference papers in civil engineering
Ernst & Sohn A Wiley Brand

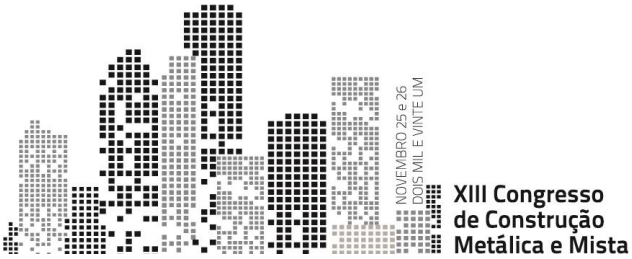

NUMERICAL INVESTIGATION OF STEEL-LVL TIMBER COMPOSITE BEAMS

Alfredo Romero [a,*], Jie Yang [b], François Hanus [c], Christoph Odenbreit [d]

[a,b,d] *University of Luxembourg, Department of Engineering. ArcelorMittal Chair of Steel Construction*
[c] *Structural Long Products, ArcelorMittal Global R&D, Luxembourg (Esch-sur-Alzette)*

Abstract: In the last years, new connectors of steel-concrete composite flooring systems have been developed and investigated to enhance the circularity and standardisation of building components. Recent studies showed that timber can be used as an alternative to the concrete slab in hybrid structures. However, the knowledge in steel-timber composite flooring systems is still very limited. This contribution presents numerical investigations of steel-LVL timber composite beams. The load deformation behaviour was determined through 3D finite element models. The design resistance of the composite beams was estimated analytically through a strain-controlled approach. The results of this study show that the resistances obtained in the numerical models and the strain-controlled approach are in good agreement. Moreover, obtained deflections and slip values were given at ultimate load.

1. Introduction

Steel is mostly used in combination with concrete in hybrid structures and one of the issues of steel-concrete composite (SCC) construction is that at the end-of-life the separation of concrete and steel is difficult and, in some cases, not feasible. Disassembly of components for easy reuse or recycling of full members is eliminated leaving only the option of demolition which means the reuse potential of structural elements is lost.
With regards to demountable and reusable structures, in the last years, new connectors for SCC flooring systems have been developed and investigated to enhance the circularity and standardisation of building components [1]. For example in the RFCS research project REDUCE [2], demountable composite beams and their shear connection were investigated and analytical calculation approaches were developed.
In addition, steel-timber composite (STC) flooring systems have been investigated experimentally and numerically. The investigations study the load-slip behaviour and failure modes of STC shear connections, Loss et al. [3] and Hassanieh et al. [4]–[8] are among the researchers

that have conducted these investigations. A few four-point and six-point bending tests and numerical studies [9]–[12] demonstrate that the bending capacity of the STC structures can be at similar levels of SCC systems. These studies implement engineered timber slabs (e.g. laminated veneer lumber, LVL) and the shear connectors investigated are screws, bolts and a combination of these with other mechanical devices and epoxy glue. Moreover, there are studies about the environmental benefits of timber slabs [13]–[15].
The existing research shows that timber can be used as an alternative to concrete slabs. Nonetheless, more research is needed to characterize the load-deformation behaviour of STC flooring systems and to develop practical design procedures. But even though the use of bolts and screws allow for deconstruction of STC structures, the drilling effect of the screws and the preloading of bolts cause permanent damages on the timber. Hence, shear connection solutions well suited for disassembly and reuse are to be developed and investigated with the target to establish reliable design methods.
This contribution presents first results of numerical investigations of steel-LVL timber composite beams under certain assumptions. First, the load-slip behaviour of a STC shear connection system for deconstruction and reuse is determined analytically according to Eurocodes [16]–[18] and implemented in a finite element (FE) model in order to study the load deformation behaviour at design level of STC beams with different geometries. In addition, the design resistance of these beams was estimated through an iterative strain-controlled approach under elastic-plastic assumptions for the material properties. Finally, the results of the FE models and the analytical calculations were compared.

2. Shear connection

The shear connection of steel-timber composite flooring systems is usually achieved by means of screws, bolts and a combination of these with other mechanical devices or glue. Connections with screws and bolts have the potential of being disassembled, however, when removing the screws, the timber is damaged and in bolted connections, the preloading can crush the timber in the vicinity of the bolt [5]. Therefore, the reuse of these timber slabs is not an option anymore because the resistance and safety of the connection cannot be guaranteed under these circumstances.
One way to cope with these issues is by reinforcing the hole of a bolted connection with a steel tube (see Fig. 1). With the tube, higher preload is achieved while preventing compressive stresses on the timber and crushing due to the preloading of the bolt, furthermore, it leads to an additional slip resistance.

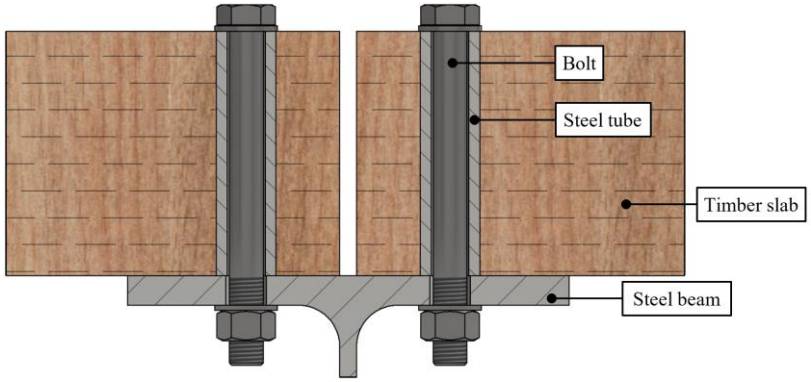

Fig. 1: Schematic representation of the bolt-in-tube connection.

The numerical investigation bases on the assumption of a load slip behaviour of the shear connection as shown in Fig. 2 and Fig. 3. A bolted connection is used to transfer the shear forces

between the slab and the steel beams. The load-slip behaviour of these connections is characterized by a curve that can be generalized as shown in Fig. 2. The first branch corresponds to the slip resistance (1) due to the preload of the bolt, when the friction is overcome, slip occurs in the bolt hole (2). Finally, the bolt gets in contact with the inner surface of the hole and bearing and shear deformation occurs (3).

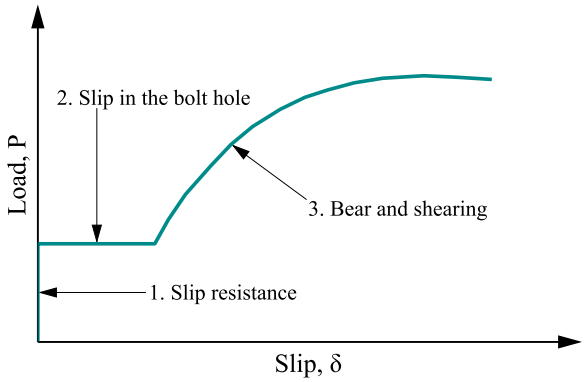

Fig. 2: Load-slip curve of a typical bolted steel-to-concrete connection [19].

On basis of the currently available information, the values for initial stiffness and slip are based on the REDUCE results and branch 3 (see Fig. 2) on Eurocode 5. Similarly to SCC bolted connections, the load-slip response of the demountable bolt-in-tube connection (see Fig. 3) is expected to have an initial slip resistance (1), followed by slip in the bolt hole (2), crushing of the timber and later bearing (3) and shear failure of the bolt (4). The load-slip response of the connection is obtained analytically as summarized in Table 1 and shown in Fig. 3. The resistance is calculated for the bolted connection shown in Fig. 1, consisting of a LVL slab class 36 C, a bolt M20 class 10.9, a steel tube class S460 with a diameter of 35 mm and a wall thickness of 6.3 mm, and a hole in the steel beam with a diameter of 24 mm.

Table 1: Slip and force values of the load-slip curve

No.	*Slip, δ [mm]*	*Load, P [kN]*
1	$0 \leq \delta < 0.5$	$\frac{F_{s,Rd}}{0.5}\delta$
2	$0.5 \leq \delta < d_0 - d$	$F_{s,Rd}$
3	$d_0 - d \leq \delta < d_0 - d + \frac{P - F_{s,Rd}}{K}$	$K(\delta - d_0 + d) + F_{s,Rd}$
4	$d_0 - d + \frac{P - F_{s,Rd}}{K} \leq \delta \leq \infty$	$P_{Rd} = F_{s,Rd} + F_{v,Rd}$

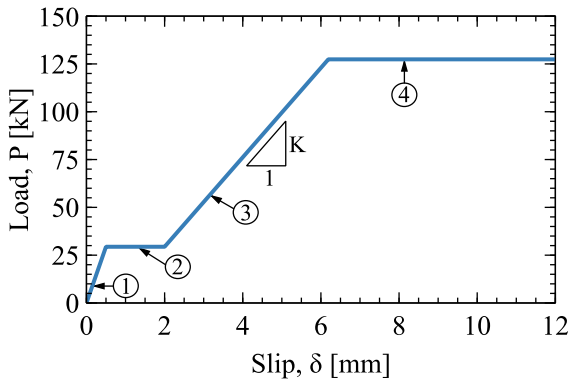

Fig. 3: Load-slip curve for the proposed connection.

In Fig. 3 the analytically obtained curve represents the load-slip response of the connection at design level estimated according to Eurocodes. The slip resistance $F_{s.Rd}$, the stiffness of the steel-to-timber connection K and the shear resistance of the bolt $F_{v,Rd}$ are estimated according to equations (1), (2) and (3) respectively.

$$F_{s.Rd} = \frac{\mu \cdot f_{ub} \cdot A_s}{\gamma_M} \quad (1)$$

$$K = \frac{4 \cdot \rho_m \cdot d_s}{69} \quad (2)$$

$$F_{v,Rd} = \frac{0.5 \cdot f_{ub} \cdot A_s}{\gamma_M} \quad (3)$$

3. Finite element modelling

3.1 General

The presented FE model bases principally on the modelling approach presented by Vigneri et al. [20] for SCC beams with the necessary changes for the implementation of timber. The steel-timber composite beam system shown in Fig. 4 was modelled using the 3D finite element software ABAQUS [21].
Only simply supported beams with uniform distributed load (UDL), were investigated all material properties implemented in the finite element model are the design properties according to Eurocodes [16]–[18]. In case, later experimental test results exist the material values out of these tests will be used for comparison. The current numerical investigation delivers however, first results about the "design resistance" values and the beam behaviour in that design case when the material strength is on its real lower limit, the design value.
The components of the model are: the LVL slab, steel beam and shear connectors. The LVL slab and the steel beam were modelled through three-dimensional 4-point reduced integration shell elements (S4R) and the shear connectors were modelled as mesh independent fasteners.

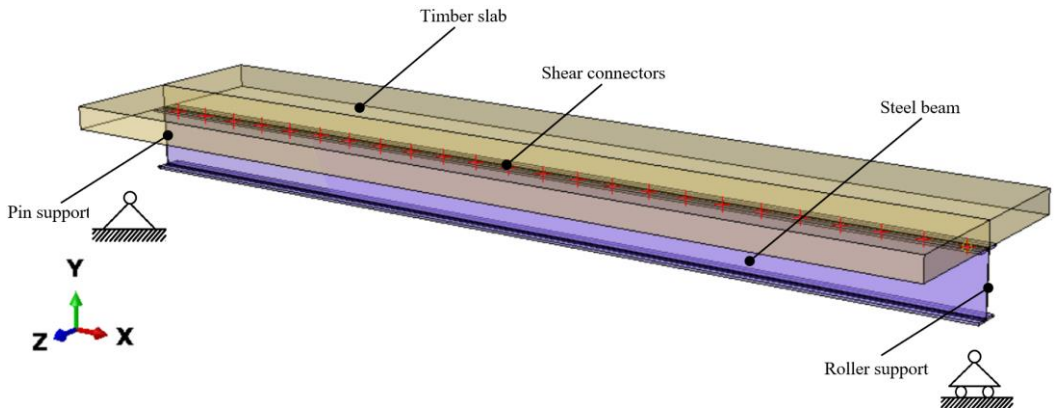

Fig. 4: 3D finite element model of a steel-timber composite beam.

Fig. 5 shows the layout of the simply supported composite beam and
Table 2 presents a summary of the configurations analysed in this study for different degrees of shear connection η (i.e. 1.0, 0.8, 0.6, 0.4, 0.2 and 0.0).

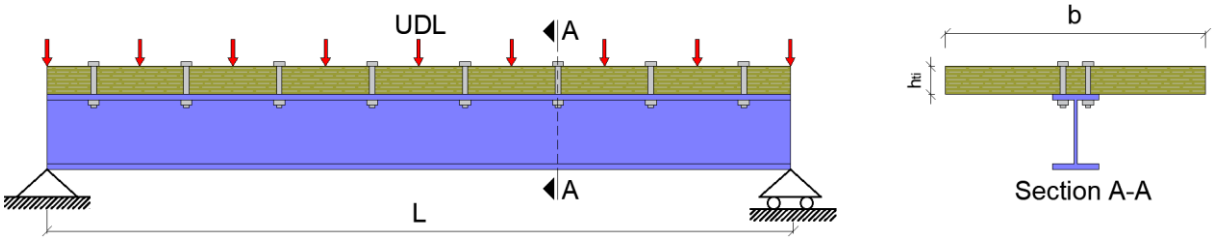

Fig. 5: Structural system of the simply supported beam under uniformly distributed load.

Table 2: Summary of steel-timber composite beams analysed in this study.

No	*Configuration*	*Length [m]*	*Steel section*	*Steel grade*	*LVL class*	*Slab height, h_{ti} [mm]*	*Slab width, b [m]*
1	6-IPE300-LVL144	6	IPE 300	S355	36 C	144	1.5
2	6-IPE300-LVL102	6	IPE 300	S355	36 C	102	1.5
3	9-IPE360-LVL144	9	IPE 360	S355	36 C	144	2.25
4	9-IPE360-LVL102	9	IPE 360	S355	36 C	102	2.25
5	12-IPE400-LVL144	12	IPE 400	S355	36 C	144	2.7
6	12-IPE400-LVL102	12	IPE 400	S355	36 C	102	2.7
7	15-IPE500-LVL144	15	IPE 500	S355	36C	144	3.75
8	15-IPE500-LVL102	15	IPE 500	S355	36C	102	3.75

3.2 Material properties and shear connection

3.2.1 Timber

The timber slab was modelled with shell (S4R) elements assuming properties of LVL class 36C reported by the manufacturer [22], considering the orientation of the grain aligned with the longitudinal axis of the beam as well as the same elasticity and strength in compression and tension. A bilinear stress strain relationship was implemented for compression and a linear relationship for tension as shown in Fig. 6. The design strength values were calculated according to Eurocode 5 assuming service class 1 and the strength modification factor k_{mod} equal to 0.8. The elasticity modulus $E_{0,d}$ was defined as 8 750 MPa, both the compressive strength $f_{cd,0}$ and the tensile strength $f_{td,0}$ as 17.33 MPa and the Poisson's ratio ν as 0.48.

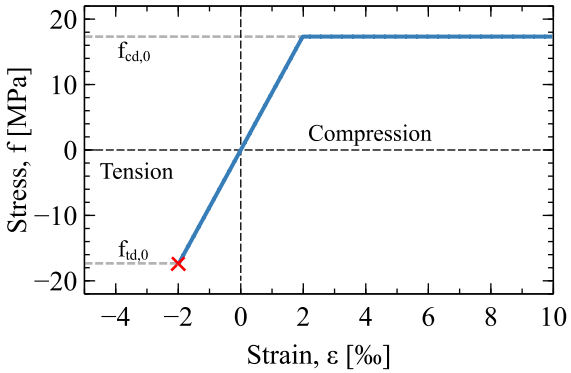

Fig. 6: Design stress-strain curves for LVL class 36 C.

3.2.2 Steel

The steel beam was modelled with shell (S4R) elements with the properties of structural steel S355. A bilinear stress-strain relationship was implemented as shown in Fig. 7. The elasticity modulus E_s was set to 210 000 MPa while the Poisson's ratio ν was taken as 0.3 and the yield strength f_{yd} as 355 MPa.

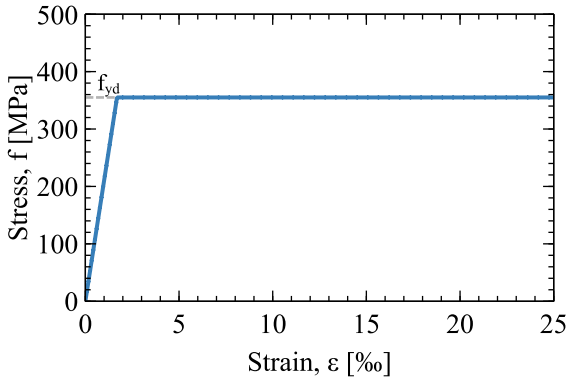

Fig. 7: Design stress-strain curves for steel grade S355.

3.2.3 Shear connection

To achieve composite action between the slab and the steel beam, two rows of equidistant shear connectors were modelled through mesh independent fasteners and the connector section of the type basic with the translational behaviour 'Slot' and the rotational type 'Align'. In this manner, the fasteners couple the slab to the steel beam allowing only the relative displacement along their longitudinal direction.

The mechanical behaviour of the connectors was defined through a multilinear load-slip curve shown in Fig. 3. The number of connectors and the spacing between them was calculated for each configuration and degree of shear connection by following the algorithm proposed by Kozma [19] for flexible shear connectors. The parameter k_{flex} was estimated for the given connection at design level, a value of 0.69 was obtained and the corresponding effective design resistance $P_{Rd,eff}$ of the proposed connection is 88 kN.

3.3 Mesh, boundary conditions and loading procedure

3.3.1 Mesh

A sensitivity analysis was performed to determine the most efficient mesh size. The average mesh size of the steel beam was defined as 50 mm while the mesh of the slab was set as 100 mm. It was determined that a finer mesh did not change the results.

3.3.2 Boundary conditions

Two reference points located at both ends of the steel beam couple the nodes of the web. The boundary conditions of the simply supported beam were assigned to these two reference points. On one end the beam is restricted to translate in the three principal directions (i.e. X, Y and Z) whereas only the longitudinal displacement along X was allowed in the other end. The rotation around the Z axis was unrestrained on both ends.

3.3.3 Loading procedure

The load was applied as a traction load on a strip located on the surface of the top flange of the steel beam. The load direction was defined through the vector (0,-1,0). These settings ensure that the load is applied along the Y (Vertical) axis throughout the whole simulation.

3.4 Validation of the model

Following the aforementioned modelling approach, a model was developed and compared with the experimental results of one steel-timber composite beam tested in 4-point bending by Hassanieh et al. [9]. It is a simply supported composite beam with a 6 m long universal beam 250 UB 25.7. The slab is made of LVL, it has a width of 400 mm and a thickness of 75 mm. The

shear connectors are bolts M12 class 8.8. Further details of the geometries, material properties and the load slip behaviour can be found in the publications of the authors [5], [9]. As shown in Fig. 8 a good agreement in terms of load-deflection was achieved. Hence, this modelling approach was chosen for carrying out the present study.

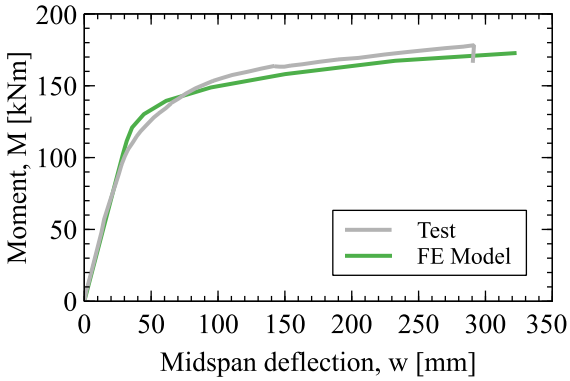

Fig. 8: Experimental and numerically obtained load-deflection curves of a STC beam tested by Hassanieh et al. [9].

4. Analytical calculation of the section resistance

4.1 Strain-controlled section resistance

On basis of the material laws given in Fig. 6 and Fig. 7 the section resistance was calculated through a strain controlled approach. This elastic-plastic analysis bases on the following assumptions: (i) timber in a composite system with steel can undergo plasticity in compression on the upper fibres; (ii) the failure of the system is governed by tensile capacity of timber; (iii) it is also assumed that the shear connectors have unlimited deformation capacity; and (iv) bi-linear stress-strain relationships for timber in compression and steel were considered, whereas for tension in timber a linear law with brittle failure is considered for the calculations.
The components were divided in several horizontal lamellas, and the corresponding stresses and forces were estimated out of the strain through an iterative approach. The strain of the bottom fibre of the timber slab was fixed as the design value of the ultimate strain of timber in tension $\varepsilon_{td,0}$ for all the cases, the strain values of the top fibre of the slab and the edge fibres of the steel beam were iterated until reaching equilibrium of forces for full and partial shear connection cases (Fig. 9).

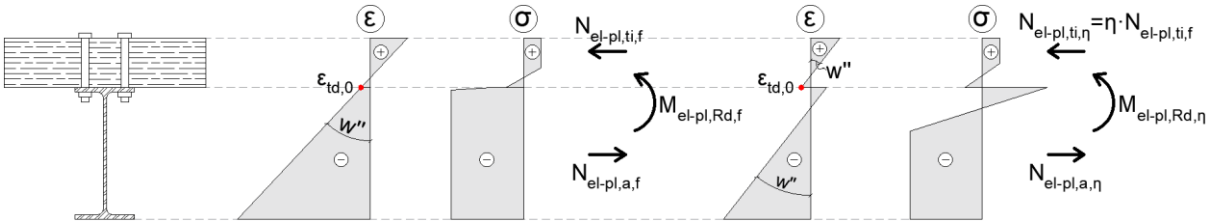

a) Bilinear stress-strain curves with full shear connection

b) Bilinear stress-strain curves with partial shear connection

Fig. 9: Strain and stress distribution for full and partial shear connection in the strain-controlled analysis.

5. Results

A comparison of the numerical and the analytical resistance values (Fig. 10) shows that there is good agreement between both. Furthermore, the midspan deflection versus moment curves were obtained from the FE models for the beams analysed in this study. Examples of the moment-midspan deflection curves of two configurations are shown in Fig. 12 and Fig. 12.

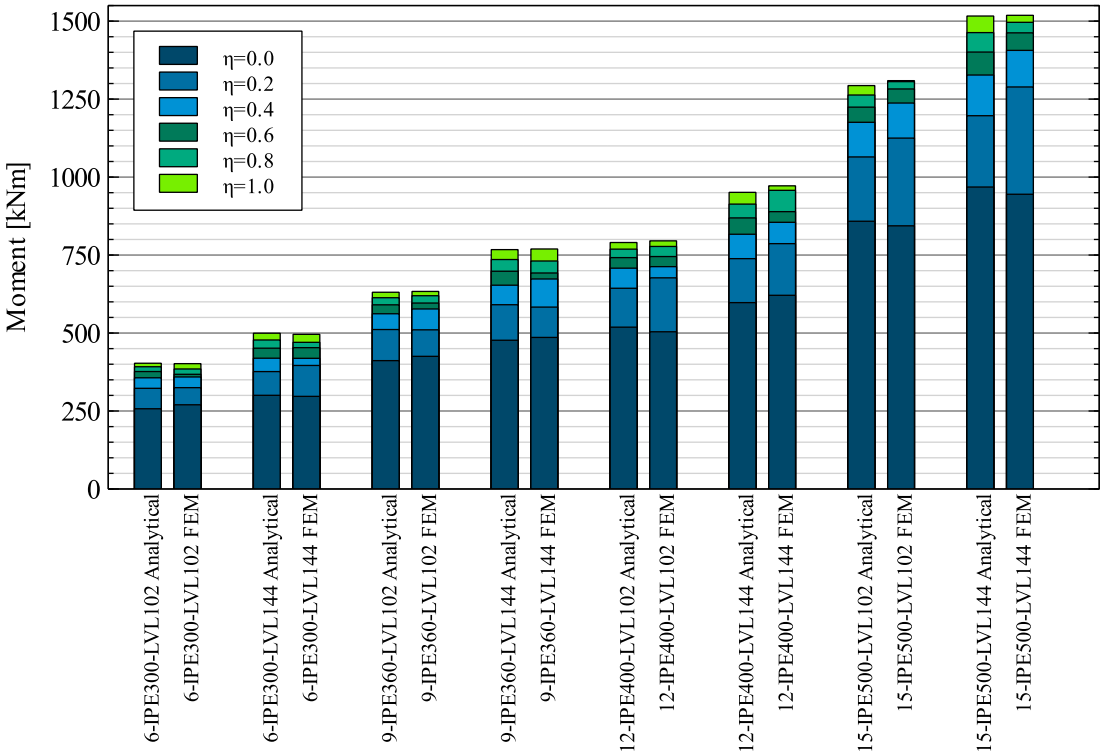

Fig. 10: Comparison of the analytically and numerically obtained resistance values.

In most cases, the slip at ultimate load is smaller than 6mm for degrees of shear connection greater than 0.6. However, large midspan deflections were observed at the ultimate load. In addition, the composite action led to a ultimate bending capacity up to 48-67% greater than the capacity of hybrid systems without shear connection.

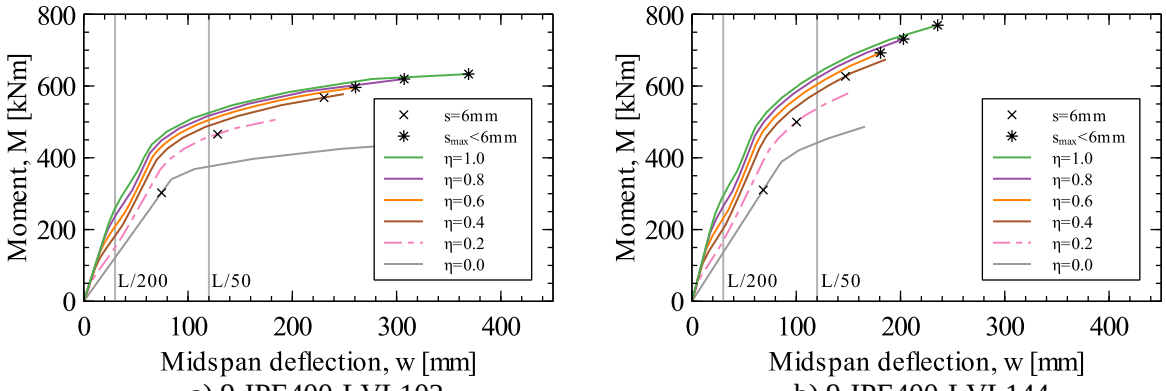

Fig. 11: Midspan deflection vs. Moment curves of beams with a span of 9m.

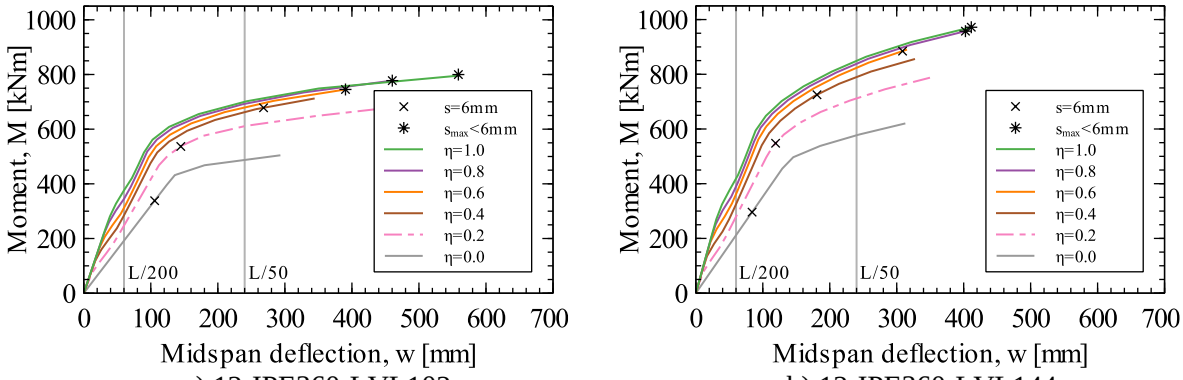

a) 12-IPE360-LVL102 b) 12-IPE360-LVL144

Fig. 12: Midspan deflection vs. Moment curves of beams with a span of 12m.

6. Conclusions

The main conclusions of the present study are as follows:

1. The use of the parameter k_{flex} to estimate the effective shear resistance and the number of connectors in the finite element model leads to resistance values that are in good agreement with the analytically obtained resistances.
2. For degrees of shear connection greater than 0.6 the slip values are smaller than 6mm, this means that the estimation of the number of connectors using the effective shear resistance proposed by Kozma [19] allows to limit the slip.
3. To reach the ultimate capacity of the steel-timber composite beams large deflections will be expected. Therefore, additional limitations may be required to ensure that deflections remain within allowable values.
4. A minimum degree of shear connection is to be established (i) to ensure an adequate increase in the bending capacity of the steel-timber composite beams compared to non-composite hybrid solutions, (ii) to maximize the utilization of the materials and (iii) to minimize deformations.

Acknowledgments

The present study was developed within the framework of the research project Prefa-SeTi. The authors gratefully acknowledge Prefalux and ArcelorMittal for their support in this partnership, and the Luxembourg's National Research Fund (FNR) for its support through the PhD Industrial Fellowship Grant No. 15695062.

References

[1] I. Jakovljević, M. Spremić, and Z. Marković, "Demountable composite steel-concrete floors: A state-of-the-art review," *Gradjevinar*, vol. 73, no. 3. 2021, doi: 10.14256/JCE.2932.2020.

[2] M. Sansom, A. Girao Coelho, R. Lawson, and et. al, "Reuse and demountability using steel structures and the circular economy (REDUCE)." Final Report, Project No. 710040, European Commission, Directorate-General for Research and Innovation, Brussels, Belgium, 2020.

[3] C. Loss, M. Piazza, and R. Zandonini, "Connections for steel–timber hybrid prefabricated buildings. Part I: Experimental tests," *Constr. Build. Mater.*, vol. 122, 2016, doi: 10.1016/j.conbuildmat.2015.12.002.

[4] A. Hassanieh, H. R. Valipour, and M. A. Bradford, “Load-slip behaviour of steel-cross laminated timber (CLT) composite connections,” *J. Constr. Steel Res.*, vol. 122, 2016, doi: 10.1016/j.jcsr.2016.03.008.

[5] A. Hassanieh, H. R. Valipour, and M. A. Bradford, “Experimental and analytical behaviour of steel-timber composite connections,” *Constr. Build. Mater.*, vol. 118, 2016, doi: 10.1016/j.conbuildmat.2016.05.052.

[6] A. Hassanieh, H. R. Valipour, and M. A. Bradford, “Composite connections between CLT slab and steel beam: Experiments and empirical models,” *J. Constr. Steel Res.*, vol. 138, 2017, doi: 10.1016/j.jcsr.2017.09.002.

[7] A. Hassanieh, H. R. Valipour, M. A. Bradford, and C. Sandhaas, “Modelling of steel-timber composite connections: Validation of finite element model and parametric study,” *Eng. Struct.*, vol. 138, pp. 35–49, 2017, doi: 10.1016/j.engstruct.2017.02.016.

[8] A. Hassanieh, H. R. Valipour, and M. A. Bradford, “Bolt shear connectors in grout pockets: Finite element modelling and parametric study,” *Constr. Build. Mater.*, vol. 176, 2018, doi: 10.1016/j.conbuildmat.2018.05.029.

[9] A. Hassanieh, H. R. Valipour, and M. A. Bradford, “Experimental and numerical study of steel-timber composite (STC) beams,” *J. Constr. Steel Res.*, vol. 122, pp. 367–378, 2016, doi: 10.1016/j.jcsr.2016.04.005.

[10] N. Keipour, H. R. Valipour, and M. A. Bradford, “Steel-timber versus Steel-Concrete Composite floors: A numerical study,” 2016.

[11] C. Loss and B. Davison, “Innovative composite steel-timber floors with prefabricated modular components,” *Eng. Struct.*, vol. 132, 2017, doi: 10.1016/j.engstruct.2016.11.062.

[12] A. Hassanieh, H. R. Valipour, and M. A. Bradford, “Experimental and numerical investigation of short-term behaviour of CLT-steel composite beams,” *Eng. Struct.*, vol. 144, 2017, doi: 10.1016/j.engstruct.2017.04.052.

[13] B. D’Amico, F. Pomponi, and J. Hart, “Global potential for material substitution in building construction: The case of cross laminated timber,” *J. Clean. Prod.*, vol. 279, p. 123487, 2021, doi: 10.1016/j.jclepro.2020.123487.

[14] O. A. B. Hassan, F. Öberg, and E. Gezelius, “Cross-laminated timber flooring and concrete slab flooring: A comparative study of structural design, economic and environmental consequences,” *Journal of Building Engineering*. 2019, doi: 10.1016/j.jobe.2019.100881.

[15] A. A. Chiniforush, A. Akbarnezhad, H. Valipour, and J. Xiao, “Energy implications of using steel-timber composite (STC) elements in buildings,” *Energy Build.*, 2018, doi: 10.1016/j.enbuild.2018.07.038.

[16] CEN, “EN 1993-1-1:2005 - Eurocode 3: Design of steel structures - Part 1-1: General rules and rules for buildings.” 2005.

[17] CEN, “EN 1993-1-8:2005 - Eurocode 3: Design of steel structures - Part 1-8: Design of joints,” 2005.

[18] CEN, “EN 1995-1-1:2004 - Eurocode 5: Design of timber structures - Part 1-1: General - Common rules and rules for buildings.” 2004.

[19] A. S. Kozma, “Demountable Composite Beams: Analytical calculation approaches for shear connections with multilinear load-slip behaviour,” University of Luxembourg, 2020.

[20] V. Vigneri, C. Odenbreit, and A. Romero, “Numerical study on design rules for minimum degree of shear connection in propped steel–concrete composite beams,” *Eng. Struct.*, vol. 241, 2021, doi: 10.1016/j.engstruct.2021.112466.

[21] D. S. Simulia, “Abaqus 6.14,” *Abaqus 6.14 Anal. User’s Guid.*, 2014.

[22] Metsä Wood, “Product Certificate.” p. 41, 2020.